Elaboration of Selective and Efficient Recognition of Thymine Base in Dinucleotides (TpT, ApT, CpT, and GpT), Single-Stranded d(GTGACGCC), and Double-Stranded d(CGCTAGCG)$_2$ by Zn^{2+}−Acridinylcyclen (Acridinylcyclen = (9-Acridinyl)methyl-1,4,7,10-tetraazacyclododecane)

Eiichi Kimura,* Hideyuki Kitamura, Kazuhiro Ohtani, and Tohru Koike

Contribution from the Department of Medicinal Chemistry, Faculty of Medicine, Hiroshima University, Kasumi 1-2-3, Minami-ku, Hiroshima 734-8551, Japan

Received January 6, 2000

Abstract: Previously, we reported that the Zn^{2+}−acridinylcyclen complex (ZnL′, acridinylcyclen = (9-acridinyl)-methyl-1,4,7,10-tetraazacyclododecane) strongly recognizes thymine base (T) in thymidine nucleoside and weakly guanine (G) in 2′-deoxyguanosine in aqueous solution (Shionoya and Kimura et al. *J. Am. Chem. Soc.* **1993**, *115*, 6730−6737; *J. Am. Chem. Soc.* **1994**, *116*, 3848−3859). In this paper, we elaborate on the ZnL′ recognition of T in dinucleotides (thymidylylthymidine (TpT), 2′-deoxyguanylylthymidine (GpT), 2′-deoxycytidylylthymidine (CpT), and 2′-deoxyadenylylthymidine (ApT)) and octanucleotides (single-stranded d(GTGACGCC) and double-stranded d(CGCTAGCG)$_2$) by means of UV spectrophotometric titration, potentiometric pH titration, ^{1}H NMR, FAB-MS measurements, and molecular modeling. The primary mode of interaction of ZnL′ with the deprotonated thymine bases (T^-) in all of these oligonucleotides was prevalent with the common affinity constants K_{app} of ca. 10^5 M^{-1} (K_{app} = [T^--bound ZnL′]/[uncomplexed ZnL′] [uncomplexed oligonucleotide]) at pH 8 and 25 °C with I = 0.10 ($NaNO_3$) regardless of the adjacent bases. The secondary mode involving $\pi-\pi$ stacking between two acridines made the synergistic binding of the two ZnL′ complexes with TpT. Thus, the second ZnL′ interaction with TpT was about 20 times more favored than the first one. The subsequent interaction of ZnL′ with G occurred to the ZnL′-bound GpT^- and d(GT^-GACGCC). The NMR study showed the double-strand destabilization of d(CGCTAGCG)$_2$ by formation of the ZnL′−T^- complex.

Introduction

Very few synthetic molecules that recognize and bind to specific nucleic acid sequences or base pairs are reported and their design to control gene expression is a challenging theme in current bioorganic and bioinorganic chemistry.[1−9] Some drugs such as bleomycin,[10−12] distamycin A,[13−19] and actinomycin D[20−24] bind to DNA with base sequence specificity. Of special interest are the compounds capable of converting duplex DNA structures at the regulatory domain of specific genes into the forms that block DNA-binding proteins (i.e., gene activators or suppressors).[25,26]

(1) Takahara, P. M.; Rosenzweig, A. C.; Frederick, C. A.; Lippard, S. J. *Nature* **1995**, *377*, 649−652.
(2) Warpehoski, M. A.; Harper, D. E. *J. Am. Chem. Soc.* **1995**, *117*, 2951−2952.
(3) Chen, H.; Olmstead, M. M.; Maestre, M. F.; Fish, R. H. *J. Am. Chem. Soc.* **1995**, *117*, 9097−9098.
(4) Iverson, B. L.; Shrender, K.; Kárl, V.; Sansom, P.; Lynch, V.; Sessler, J. L. *J. Am. Chem. Soc.* **1996**, *118*, 1608−1616.
(5) Nicolaou, K. C.; Smith, B. M.; Ajito, K.; Komatsu, H.; Gomez-Paloma, L.; Tor, Y. *J. Am. Chem. Soc.* **1996**, *118*, 2303−2304.
(6) Qu, Y.; Bloemink, M. J.; Reedijk, J.; Hambley, T. W.; Farrell, N. *J. Am. Chem. Soc.* **1996**, *118*, 9307−9313.
(7) Kuklenyik, Z.; Marzilli, L. G. *Inorg. Chem.* **1996**, *35*, 5654−5664.
(8) Boger, D. L.; Hertzog, D. L.; Bollinger, B.; Johnson, D, S.; Cai, H.; Goldberg, J.; Turnbull, P. *J. Am. Chem. Soc.* **1997**, *119*, 4977−4986.
(9) Guo, Z.; Sadlar, P. J.; Zang, E. *J. Chem. Soc., Chem. Commun.* **1997**, 27−28.
(10) Manderville, R. A.; Ellena, J. F.; Hecht, S. M. *J. Am. Chem. Soc.* **1995**, *117*, 7891−7903.
(11) Stubbe, J.; Kozarich, J. W. *Chem. Rev.* **1987**, *87*, 1107−1136.
(12) Calafat, A. M.; Won, H.; Marzilli, L. G. *J. Am. Chem. Soc.* **1997**, *119*, 3656−3664.
(13) Van Dyke, M. W.; Hertzberg, R. P.; Dervan, P. B. *Proc. Natl. Acad. Sci. U.S.A.* **1982**, *79*, 5470−5474.
(14) Van Dyke, M. W.; Dervan, P. B. *Nucleic Acids Res.* **1983**, *11*, 5555−5567.
(15) Fox, K. R.; Waring, M. J. *Nucleic Acids Res.* **1984**, *12*, 9271−9285.
(16) Coll, M.; Frederick, C. A.; Wang, A. H.-J.; Rich, A. *Proc. Natl. Acad. Sci. U.S.A.* **1987**, *84*, 8385−8389.
(17) Griffin, J. H.; Dervan, P. B. *J. Am. Chem. Soc.* **1987**, *109*, 6840−6842.
(18) Woynarowski, J. M.; Sigmund, R. D.; Beerman, T. A. *Biochemistry* **1989**, *28*, 3850−3855.
(19) Wilson, W. D.; Ratmeyer, L.; Zhao, M.; Strekowski, L.; Boykin, D. *Biochemistry* **1993**, *32*, 4098−4104.
(20) Müller, W.; Crothers, D. M. *J. Mol. Biol.* **1968**, *35*, 251−290.
(21) Solbell, H. M.; Jain, S. C.; Sakore, T. D.; Nordman, C. E. *Nat. New Biol.* **1971**, *231*, 200−205.
(22) Lane, M. J.; Dabrowiak, J. C.; Vournakis, J. N. *Proc. Natl. Acad. Sci. U.S.A.* **1983**, *80*, 3260−3264.
(23) Chu, W.; Shinomiya, M.; Kamitori, K. Y.; Kamitori, S.; Carlson, R. G.; Weaver, R. F.; Takusagawa, F. *J. Am. Chem. Soc.* **1994**, *116*, 7971−7982.
(24) Schäfer, M.; Sheldrick, G. M.; Bahner, I.; Lackner, H. *Angew. Chem., Int. Ed. Engl.* **1998**, *37*, 2381−2384.
(25) Colocci, N.; Dervan, P. B. *J. Am. Chem. Soc.* **1995**, *117*, 4781−4787.
(26) Fernandez-Saiz, M.; Schneider, H.-J.; Sartorius, J.; Wilson, W. D. *J. Am. Chem. Soc.* **1996**, *118*, 4739−4745.

10.1021/ja000083j CCC: $19.00
Published on Web 04/27/2000

Scheme 1

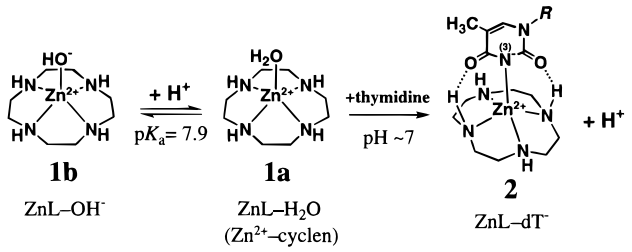

Scheme 2

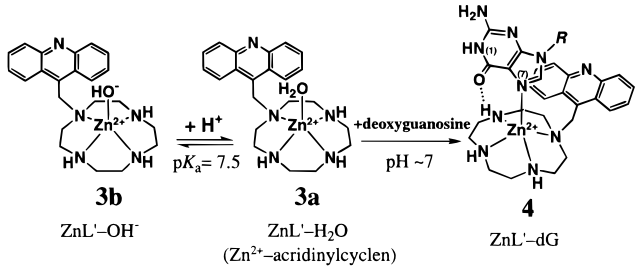

We originally discovered that Zn^{2+}−cyclen (ZnL, **1**) (cyclen = 1,4,7,10-tetraazacyclododecane), *in aqueous solution at physiological pH*, selectively binds to thymidine (dT) nucleoside and its homologues at the deprotonated imide N(3)$^-$ to form stable 1:1 complexes (e.g., see **2** (ZnL−dT$^-$) for dT (Scheme 1), K_{app} = [**2**]/[**1a** + **1b**][uncomplexed dT] = $10^{3.5}$ M^{-1} at pH 8 and 25 °C).[27] Later, its derivative Zn^{2+}−acridinylcyclen (ZnL′, **3**) (acridinylcyclen = (9-acridinyl)methyl-1,4,7,10-tetraazacyclododecane) was shown to possess a stronger affinity to thymidine (K_{app} = [ZnL′−dT$^-$]/[**3a** + **3b**][uncomplexed dT] = $10^{4.9}$ M^{-1} at pH 8 and 25 °C) and also a fairly strong binding with 2′-deoxyguanosine (dG) at guanine N(7) to yield a 1:1 ZnL′−dG complex **4** (K_{app} = [**4**]/[**3a** + **3b**][uncomplexed dG] = $10^{3.5}$ M^{-1} at pH 8 and 25 °C) (Scheme 2).[28]

Recently, such ZnL and ZnL′ interaction modes were applied to a single-stranded polynucleotide, poly(U), and double-stranded polynucleotides, poly(A)·poly(U) and poly(dA)·poly(dT).[29,30] The apparent affinity constant K_{app} of ZnL to U in poly(U) (K_{app} = [ZnL−U$^-$]/[**1a** + **1b**][uncomplexed U in poly(U)] = $10^{3.0}$ M^{-1} at pH 8 and 25 °C) was indirectly determined by inhibition kinetics of **1b**-catalyzed 4-nitrophenyl acetate hydrolysis by poly(U).[30] The interaction of ZnL′ with poly(U) in the double-stranded poly(A)·poly(U) was proposed by a comparison of CD spectra of poly(A)·poly(U), poly(A), and poly(U) in the presence of ZnL′.[29,30] Other indirect evidence for the interactions of ZnL and ZnL′ with U$^-$ was obtained by dose-dependent lowering of the melting temperature (T_m) of poly(A)·poly(U), which indicated destabilization of the duplex structure in the presence of ZnL or ZnL′.[29,30] Thus, ZnL and ZnL′ seemed to disrupt the duplex conformation of poly(dA)·poly(dT) and poly(A)·poly(U) by exclusive binding to T and U nucleobases. Moreover, ZnL′ seemed to interact with guanine (G) in poly(dG) to stabilize double-stranded poly(dG)·poly(dC) (50 μM nucleobase pair), as was suggested by the extremely raised T_m value from 73.5 °C (in the absence of ZnL′) to >95 °C (in the presence of 50 μM ZnL′).[29,30]

Scheme 3

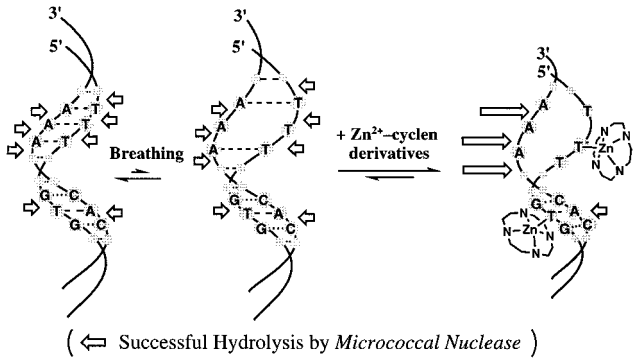

More recently, the interactions of Zn^{2+}−cyclen derivatives with native DNA (150 bp from plasmid pUC19) were studied by biochemical means, i.e., DNA footprinting assay with *micrococcal nuclease*, which qualitatively demonstrated that the Zn^{2+}−cyclen derivatives selectively bind to T to disrupt A−T hydrogen bonds (especially in homopolymeric AT-regions), but negligibly to G (see Scheme 3).[31] Furthermore, ZnL′ selectively bind to T in the TATA box of the SV40 early promoter region to inhibit the binding of a transcriptional factor (e.g., TATA box binding protein).[32] The Zn^{2+}−cyclen derivatives inhibited the DNA-directed transcription with *E. coli* RNA polymerase in vitro.[33] Thus, the small molecular Zn^{2+}−cyclen derivatives appeared to be a potential, new prototype of the genetic transcriptional regulation factor.

It is now pertinent to elaborate on the recognition of T and G in polynucleotides by ZnL′. We have studied the interaction of ZnL′ with dinucleotides, thymidylylthymidine (TpT), 2′-deoxyguanylylthymidine (GpT), 2′-deoxycytidylylthymidine (CpT), and 2′-deoxyadenylylthymidine (ApT) and single-stranded d(GTGACGCC) and double-stranded d(CGCTAGCG)$_2$ by the potentiometric pH, UV, and NMR titrations, etc. Of particular interest are (i) whether the interaction of ZnL′ with T is affected by the adjacent other nucleotides, (ii) how T and G competitively interacts with ZnL′ in GpT or the G·T-containing octanucleotides, and (iii) whether cooperative binding of ZnL′ to TpT can be verified, as so suspected from the remarkable homopolymeric AT recognition of ZnL′ in the DNA footprinting.[31]

Results and Discussion

Direct Evidence for the Interaction of Zn^{2+}−Acridinylcyclen (ZnL′) with T$^-$ and G groups in Dinucleotides and Octanucleotides by the Solution pH Change upon Mixing. When Zn^{2+}−acridinylcyclen ZnL′ **3** interacts with the thymine group (T), an equivalent proton is released from the imide N(3)H group to form ZnL′−T$^-$ (like **2** in Scheme 1). On the other hand, when **3a** interacts with the guanine group (G), no proton is released from the complex ZnL′−G (see **4** in Scheme 2). Therefore, in an unbuffered solution of 50 μM ZnL′ that is a mixture of **3a** (ZnL′−H$_2$O) and **3b** (ZnL′−OH$^-$) at initially adjusted pH 7.45 (since the pK_a value is 7.5 for ZnL′−H$_2$O ⇄ ZnL′−OH$^-$ + H$^+$, see Scheme 2), the complexation of **3a** with T should decrease the solution pH, while the complexation with G should promote the protonation of **3b** to **3a** (i.e., proton consumption) and as a result should increases the solution pH.

(27) Shionoya, M.; Kimura, E.; Shiro, M. *J. Am. Chem. Soc.* **1993**, *115*, 6730−6737.
(28) Shionoya, M.; Ikeda, T.; Kimura, E.; Shiro, M. *J. Am. Chem. Soc.* **1994**, *116*, 3848−3859.
(29) Kimura, E.; Ikeda, T.; Shionoya, M. *Pure Appl. Chem.* **1997**, *69*, 2187−2195.
(30) Kimura, E.; Ikeda, T.; Aoki, S.; Shionoya, M. *J. Biol. Inorg. Chem.* **1998**, *3*, 259−267.
(31) Kikuta, E.; Murata, M.; Katsube, N.; Koike, T.; Kimura, E. *J. Am. Chem. Soc.* **1999**, *121*, 5426−5436.
(32) Kikuta, E.; Koike, T.; Kimura, E. *J. Inorg. Bio. Chem.* In press.
(33) Kikuta, E.; Katsube, N.; Kimura, E. *J. Biol. Inorg. Chem.* **1999**, *4*, 431−440.

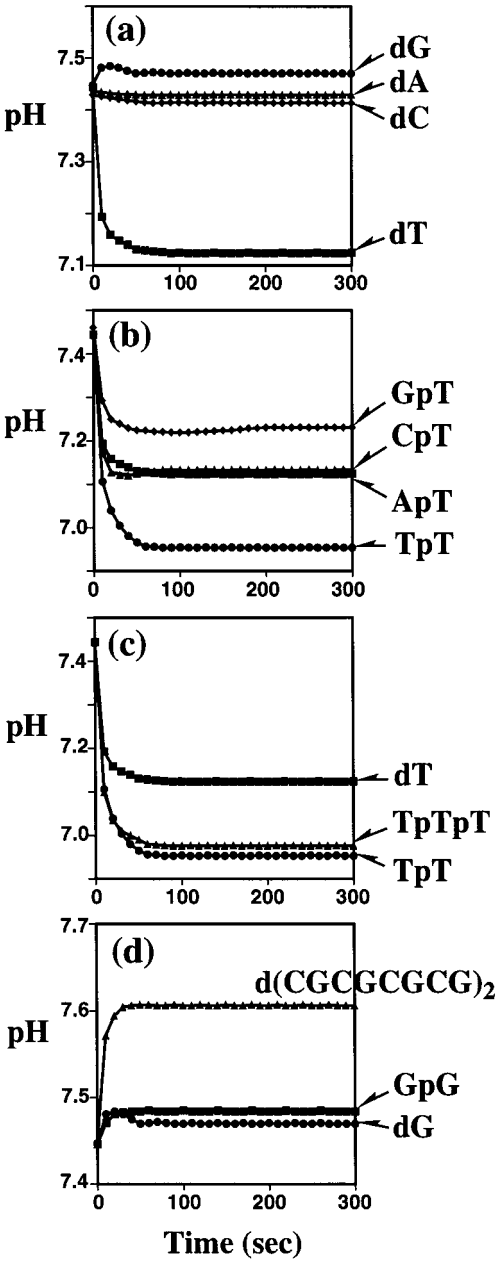

Figure 1. The pH changes of the unbuffered solution of ZnL′ **3** (50 μM, pH 7.45 at 25 °C with $I = 0.10$ ($NaNO_3$)) upon addition of 2′-deoxynucleosides (50 μM) and oligonucleotides (all containing 50 μM T or 50 μM G).

Consequently, the direct observation of the extent of the complexation would be possible by measuring the pH change upon mixing of ZnL′ with 2′-deoxynucleosides (or oligonucleotides).

We initially tested the pH change with 2′-deoxynucleosides (see Figure 1a). We repeated all the following experiments three times to see all reproducible results. To an unbuffered solution (pH 7.45) of 50 μM ZnL′ ([**3a**]/[**3b**] = ca. 1) at 25 °C with $I =$ 0.10 ($NaNO_3$) was added equimolar amounts of thymidine (dT). Indeed, we saw a pH drop to 7.12. When an equimolar amount of 2′-deoxyguanosine (dG) was added to 50 μM ZnL′, the solution pH increased to 7.47, although not as significantly as the pH decrease by dT (reflecting a weaker ZnL′−G association). By contrast, 2′-deoxycytidine (dC) and 2′-deoxyadenosine (dA) showed negligible pH changes, a fact supporting the notion that ZnL′ practically did not interact with dC and dA.

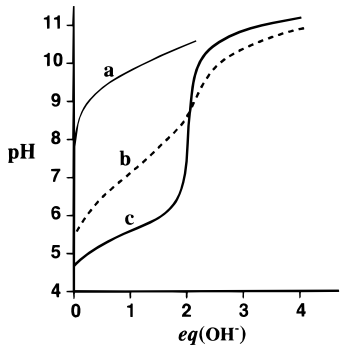

Figure 2. Potentiometric pH titration curves at 25 °C with $I = 0.10$ ($NaNO_3$): (a) 1 mM TpT; (b) 1 mM TpT + 2 mM **1**; and (c) 1 mM TpT + 2 mM **3**. eq(OH^-) is the number of equivalents of base added.

We then added dinucleotides, TpT (25 μM), GpT (50 μM), CpT (50 μM), or ApT (50 μM) (i.e., [total T] = 50 μM in any dinucleotide), to an unbuffered solution of 50 μM ZnL′ under the same conditions as used for 2′-deoxynucleosides (see Figure 1b). The extent of the pH decrease (to 6.95) by 25 μM TpT was larger than that (to 7.12) by 50 μM dT, suggesting a cooperative binding of the two ZnL′ to TpT (vide infra). With CpT and ApT, the pH values went down (to 7.13 and 7.12, respectively) to almost the same extent as with dT, indicating that ZnL′ bound to the thymine group in CpT and ApT as strongly as to dT. With 50 μM GpT, the pH decrease (to 7.23) was not as extensive as with 50 μM dT, suggesting that some portion of ZnL′ went to bind to G. Among thymidine nucleoside and nucleotides, dT (50 μM), TpT (25 μM), and thymidylylthymidylylthymidine (TpTpT, 16.7 μM) (i.e., [total T] = 50 μM in all), TpT brought the biggest pH drop (see Figure 1c), leading to a suggestion that *ZnL′ most favorably bound to the two consecutive thymine bases in TpT*, possibly due to a synergistic effect particular to the $(ZnL')_2-T^-pT^-$ complex. To compare the ZnL′ binding affinities to the G group in deoxyguanosine (dG), dinucleotide GpG, and double-stranded octanucleotide $d(CGCGCGCG)_2$, dG (50 μM), GpG (25 μM), or $d(CGCGCGCG)_2$ (6.25 μM) (i.e., [total G] = 50 μM) was added to an unbuffered solution of ZnL′ (50 μM) (see Figure 1d). The order of the solution pH increase by the ZnL′−G complex formation was $d(CGCGCGCG)_2$ > GpG > dG. It was thus concluded that ZnL′ bound to G increasingly favorably to GpG and the double-stranded $d(CGCGCGCG)_2$, for which the $\pi-\pi$ stacking contribution by the acridine pendant would account.

Potentiometric pH Titrations of ZnL (1) and ZnL′ (3) with Thymidylylthymidine (TpT). The synergistic effect in the interaction of TpT with 2 equiv of ZnL′ (**3**) was quantitatively assessed by potentiometric pH titrations with $I = 0.10$ ($NaNO_3$) at 25 °C.[27,28] Typical pH titration curves for TpT (1.0 mM) in the absence (Figure 2a) and presence of **1** (2.0 mM, Figure 2b) or **3** (2.0 mM, Figure 2c) are shown. The two imide deprotonation constants for TpT are 9.55 and 10.25.[34] The buffer pH regions at 0 < eq(OH^-) < 2 in the presence of **1** or **3** significantly dropped, which suggested the successive deprotonations from the two thymidyl imide N(3)H for the complexation with **1** or **3** to form the final $(ZnL)_2-T^-pT^-$ **6** or $(ZnL')_2-T^-pT^-$ **8**, respectively (see Schemes 4 and 5). The decrease in the buffer pH was more significant and the neutralization break at eq(OH^-) = 2 was sharper with **3** than those with **1**, indicating that TpT formed a more stable complex with 2 equiv of **3** than with 2 equiv of **1**.

(34) Kimura, E.; Kikuchi, M.; Kitamura, H.; Koike, T. *Chem. Eur. J.* **1999**, *5*, 3113−3123.

Scheme 4

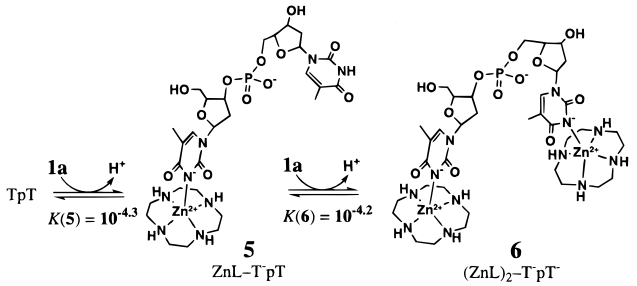

Scheme 5

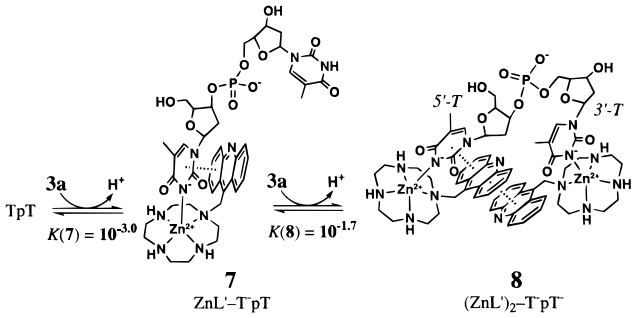

The complexation equilibria for the mixture of ZnL **1** (2 mM) and TpT (1 mM) in Figure 2b were analyzed by the program "BEST",[35] where the 1:1 and 2:1 complexes (**5** and **6**, respectively) were defined by eqs 1 and 2. The log K(**5**) and log K(**6**) values were estimated to be -4.3 ± 0.1 and -4.2 ± 0.1, respectively. Both the complexation constants are almost the same as the reported value (log K(**2**)) of -4.2 for the ZnL$-$dT$^-$ complex (K(**2**) = [**2**]a_{H^+}/[ZnL][dT]),[27] which indicates almost independent binding of ZnL to each thymine unit.[36]

$$\mathbf{1a} + \mathrm{TpT} \rightleftarrows \mathrm{ZnL{-}T^{-}pT}\ (\mathbf{5}) + \mathrm{H^+}$$
$$K(\mathbf{5}) = [\mathbf{5}]a_{\mathrm{H^+}}/[\mathbf{1a}][\mathrm{TpT}] \quad (1)$$

$$\mathbf{1a} + \mathbf{5} \rightleftarrows (\mathrm{ZnL})_2{-}\mathrm{T^{-}pT^{-}}\ (\mathbf{6}) + \mathrm{H^+}$$
$$K(\mathbf{6}) = [\mathbf{6}]a_{\mathrm{H^+}}/[\mathbf{1a}][\mathbf{5}] \quad (2)$$

When a mixture of ZnL′ **3** (2 mM) and TpT (1 mM) was titrated (Figure 2c), the pH titration data approximately fit to eq 5, i.e., simultaneous complexation of two ZnL′ with TpT to form the single 2:1 complex **8**. The complexation constant log K'(**8**) value of -5.0 ± 0.2 was obtained by ignoring **7** as a very minor species. Then, the titration of ZnL′ **3** (1 mM) with TpT (1 mM) was conducted to study the more detailed stepwise complexations to ZnL′$-$T$^-$pT **7** (equation 3) and the following (ZnL′)$_2-$T$^-$pT$^-$ **8** (eq 4), which gave log K(**7**) and log K(**8**) values of -3.0 ± 0.1 and -1.7 ± 0.1, respectively (see Scheme 5). Both values were larger than the corresponding values of -4.3 and -4.2 for ZnL **1**, indicating stronger complexations. The most interesting of all was that *the second ZnL′ complexation (from **7** to **8**) was about 20 times more favorable than the first ZnL′ complexation (to **7**)*, a fact quantitatively supporting the synergistic effect in the complexation of ZnL′ with TpT. The calculated log K'(**8**) value of -4.7 (=log K(**7**) + log K(**8**)) would be more accurate than the above log K'(**8**) value of -5.0.

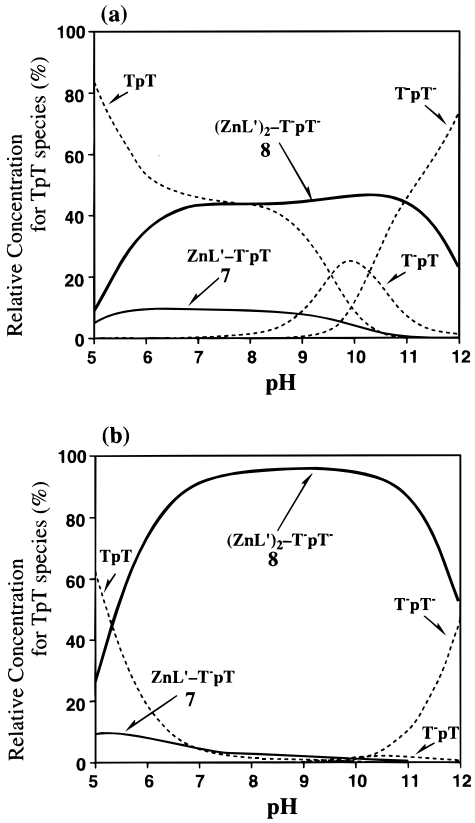

Figure 3. The pH-dependent distribution diagrams at 25 °C with I = 0.10 ($NaNO_3$): (a) 1 mM TpT and 1 mM ZnL′ **3** and (b) 1 mM TpT and 2 mM ZnL′ **3**.

$$\mathbf{3a} + \mathrm{TpT} \rightleftarrows \mathrm{ZnL'{-}T^{-}pT}\ (\mathbf{7}) + \mathrm{H^+}$$
$$K(\mathbf{7}) = [\mathbf{7}]a_{\mathrm{H^+}}/[\mathbf{3a}][\mathrm{TpT}] \quad (3)$$

$$\mathbf{3a} + \mathbf{7} \rightleftarrows (\mathrm{ZnL'})_2{-}\mathrm{T^{-}pT^{-}}\ (\mathbf{8}) + \mathrm{H^+}$$
$$K(\mathbf{8}) = [\mathbf{8}]a_{\mathrm{H^+}}/[\mathbf{3a}][\mathbf{7}] \quad (4)$$

$$2(\mathbf{3a}) + \mathrm{TpT} \rightleftarrows (\mathrm{ZnL'})_2{-}\mathrm{T^{-}pT^{-}}\ (\mathbf{8}) + 2\mathrm{H^+}$$
$$K'(\mathbf{8}) = [\mathbf{8}](a_{\mathrm{H^+}})^2/[\mathbf{3a}]^2[\mathrm{TpT}] \quad (5)$$

The pH-dependent speciation diagrams for TpT (1 mM) and ZnL′ **3** (1 mM and 2 mM) were calculated as a function of pH using the obtained K(**7**), K(**8**), and pK_a value for **3a** ⇄ **3b** and TpT to obtain Figure 3a,b. The synergistic binding of ZnL′ to TpT was well illustrated by the much higher distribution of **8** (>40%) than **7** (<10%) with an equimolar amount of ZnL′ (Figure 3a). With 2 equiv of ZnL′ more than 90% of the species was (ZnL′)$_2-$T$^-$pT$^-$ complex **8** at physiological pH (see Figure 3b).

In Figure 1c, we saw 50 μM ZnL′ **3** more favorably bound to 25 μM TpT than to 50 μM dT. To substantiate this, we performed potentiometric pH titrations of ZnL′ **3** (1 mM) in the presence of dT (1 mM) or TpT (0.5 mM) under the same conditions (see Figure 4d,e). From a comparison of the extent of the decrease in pH for the imide deprotonation, it is immediately convincing that TpT is a better ligand than 2 equiv of dT for ZnL′ (see Figure 4a → e and b → d).

We also have determined the complexation constants of ZnL′ **3** (1 mM) with CpT (1 mM) and ApT (1 mM) by the

(35) Martell, A. E.; Motekaitis, R. J. *Determination and Use of Stability Constants*, 2nd ed.; VCH: New York, 1992.

(36) The initial 1:1 complexes **5** and the following **7** were provisionally written as ZnL$-$T$^-$pT (or ZnL′$-$T$^-$pT), although the location of ZnL (or ZnL′) was not identified.

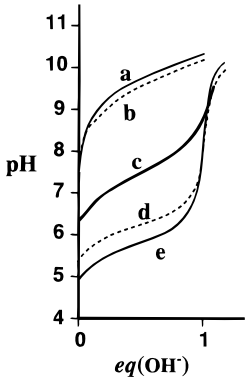

Figure 4. Potentiometric pH titration curves at 25 °C with $I = 0.10$ ($NaNO_3$): (a) 0.5 mM TpT; (b) 1 mM dT; (c) 1 mM **3**; (d) 1 mM dT + 1 mM **3**; and(e) 0.5 mM TpT + 1 mM **3**. eq(OH^-) is the number of equivalents of base added.

potentiometric pH titration at 25 °C with $I = 0.10$ ($NaNO_3$) (see eqs 6 for ZnL′−CpT^- **9** and 7 for ZnL′−ApT^- **10**). The

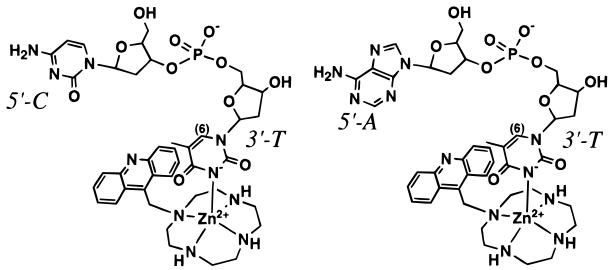

9 ZnL'–CpT^- **10** ZnL'–ApT^-

thymine-imide deprotonation constants for CpT and ApT were determined to be 9.80 ± 0.05 and 10.00 ± 0.05, respectively. The calculated log K(**9**) and log K(**10**) values were both the same value of −2.8 ± 0.1, which were close to log K(ZnL′−dT^-) of −2.5 for the 1:1 ZnL′−dT^- complex, where K(ZnL′−dT^-) = [ZnL′−dT^-]a_{H^+}/[**3a**][dT].[28] This result is consistent with almost the same extent of the pH decreases shown in Figure 1b.

$$\mathbf{3a} + \mathrm{CpT} \rightleftarrows \mathrm{ZnL'{-}CpT^-}\ (\mathbf{9}) + \mathrm{H^+}$$
$$K(\mathbf{9}) = [\mathbf{9}]a_{\mathrm{H^+}}/[\mathbf{3a}][\mathrm{CpT}] \quad (6)$$

$$\mathbf{3a} + \mathrm{ApT} \rightleftarrows \mathrm{ZnL'{-}ApT^-}\ (\mathbf{10}) + \mathrm{H^+}$$
$$K(\mathbf{10}) = [\mathbf{10}]a_{\mathrm{H^+}}/[\mathbf{3a}][\mathrm{ApT}] \quad (7)$$

The complexation of ZnL′ with GpT could not be assessed by the pH−metric titration because of the mixed pH responses of G (pH raising) and T (pH lowering).[28]

UV Spectrophotometric Titration of ZnL′ (3) with Dinucleotides TpT, GpT, CpT, and ApT. The involvement of the acridine pendant in the complexations between ZnL′ **3** and the T-containing dinucleotides was studied by the UV spectrophotometric titrations of **3** (2.0 mM, $\lambda_{max} = 362$ nm, $\epsilon = 9.22 \times 10^3$ (M^{-1} cm^{-1}), due to the acridine chromophore) with 0−3 mM dinucleotides or dT (for reference) at pH 8.4 (20 mM TAPS buffer) and 25 °C with $I = 0.10$ ($NaNO_3$). Earlier, we found that due to the $\pi-\pi$ stacking interaction of the acridine with thymine, the ZnL′−dT^- complexation caused the hypochromic effect on the acridine UV absorption.[33]

The titrations with dT, CpT, and ApT gave almost the same linear declines in the UV absorption at 362 nm unitl equimolar

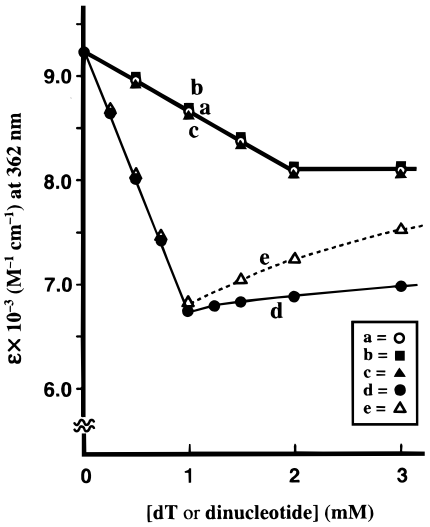

Figure 5. UV spectrophotometric titrations (at 362 nm) of ZnL′ **3** (2 mM) at 25 °C in pH 8.4 (20 mM TAPS buffer) with $I = 0.10$ ($NaNO_3$): (a) dT (0−3 mM); (b) ApT (0−3 mM); (c) CpT (0−3 mM); (d) TpT (0−3 mM); and (e) GpT (0−3 mM). The ϵ values of the test solutions are for the acridine group of **3**.

additions (Figure 5a−c). Thus, the complexations for ZnL′−dT^-, ZnL′−CpT^- (**9**), and ZnL′−ApT^- (**10**) under the experimental conditions are stoichiometric. A break was seen at equimolar amounts of dT, ApT, and CpT ($\epsilon = 8.11 \times 10^3$ for ZnL′−dT^-, 8.13×10^3 for ZnL′−ApT^-, and 8.08×10^3 for ZnL′−CpT^-, respectively). In the case of 0−3 mM TpT and GpT addition (see Figure 5d,e), the results indicated an overlapping steeper slope, which was due to the simultaneous formation of 2:1 complexes $(ZnL')_2$−T^-pT^- **8** ($\epsilon = 6.71 \times 10^3$) and $(ZnL')_2$−GpT^- (6.83×10^3) **11**. The greater hypochromic

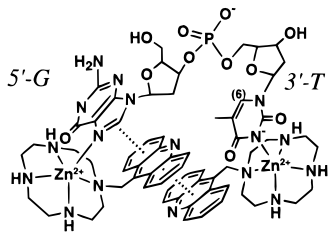

11 $(ZnL')_2$–GpT^-

effects of the 2:1 complexes $(ZnL')_2$−T^-pT^- and $(ZnL')_2$−GpT^- than those of ZnL′−dT^-, −ApT^-, and −CpT^- probably arose from a face-to-face $\pi-\pi$ stacking of the two acridine moieties in the 2:1 complexes (vide infra). The hypochromic effect became reduced as [GpT] went beyond 1 mM (Figure 5e), which implied that the equilibrium between ZnL′ and GpT shifted to the more favorable 1:1 ZnL′−GpT^- complex, whereby the ϵ value became closer to that for the ZnL′−dT^- complex.

NMR Titration of Dinucleotides with ZnL′ (3). The synergistic formation of the 2:1 $(ZnL')_2$−T^-pT^- complex **8** in a mixture of TpT (1 mM) and **3** (1 mM) (e.g., Figure 3a) was confirmed by the ^{1}H NMR titration of TpT (5 mM) with **3** (0−10 mM) in D_2O at 25 °C and pD 8.4. Assignments of all the protons in TpT and the 2:1 complex **8** were made by means of two-dimensional COSY and ROESY experiments. These studies permitted unambiguous assignment of the 5′- and 3′-thymine base HC(6) protons as each showed a ROE between HC(6) of T and HC(2′) of the sugar. The aromatic protons of the acridine

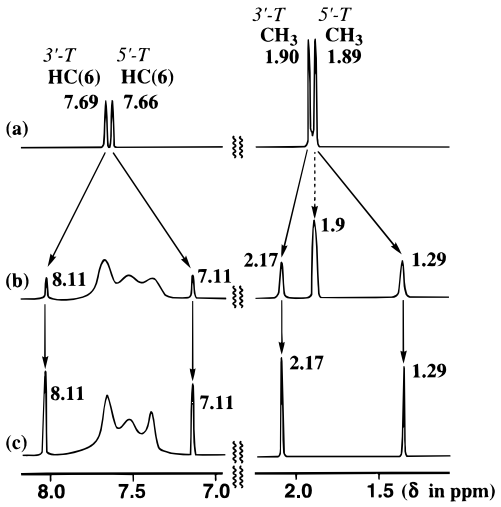

Figure 6. ^{1}H NMR spectra at pD 8.4 and 25 °C in D_2O: (a) 5 mM TpT; (b) 5 mM TpT + 5 mM **3**; and (c) 5 mM TpT + 10 mM **3**.

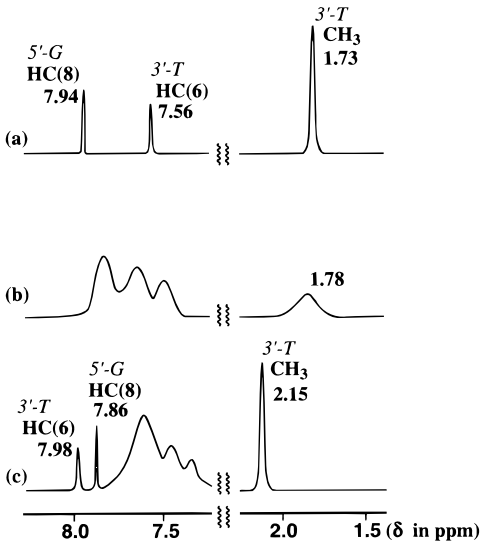

Figure 7. ^{1}H NMR spectra at pD 8.4 and 25 °C in D_2O: (a) 5 mM GpT; (b) 5 mM GpT + 5 mM **3**; and (c) 5 mM GpT + 10 mM **3**.

moiety of **3** occurred as four strong peaks in the range δ 7.5−8.1 in D_2O at 25 °C.[28] When **3** (5 mM) was added to TpT (5 mM), about half of the CH_3−C(5) protons (δ 1.89) and the aromatic HC(6) proton (δ 7.66) of 5′-T moved upfield to 1.29 and 7.11, respectively (see Figure 6). On the other hand, the chemical shifts of the corresponding protons on 3′-T moved downfield from δ 1.90 to 2.17 and from δ 7.69 to 8.11, respectively. These chemical shifts indicated the formation of the 2:1 complex **8** with negligible intermediary of the 1:1 complex **7**. The upfield shifts of the T$^-$ protons were also observed with the ZnL′−dT$^-$ complex, in which the acridine pendant was confirmed to stack to T$^-$ by the X-ray crystal strucutre.[28] Therefore, we have concluded that in **8**, 5′-T was stacked with an acridine. On the other hand, the downfield shifts of the 3′-T protons were thought to be due to the deshielding effect of the other acridine. The protons of two acridine rings in **8** were too broadened to be assigned at δ 7−8. All these data combined, and it was proposed that the two acridine moieties were arrayed face-to-face and 5′-T stacked to one of these, while 3′-T laid down orthogonally against the other acridine. Such a proposed structure for **8** was supported by the following FAB mass spectral and molecular modeling studies.

To check the 2:1 $(ZnL')_2$−GpT$^-$ **11** complexation, as postulated by the UV spectrophotometric titration, GpT (5 mM) (Figure 7a) was mixed with **3** (5 mM) at 25 °C, whereupon the CH_3−C(5) protons of 3′-T (δ 1.73) were broadened and moved downfield to 1.78 (Figure 7b), and the HC(6) proton of 3′-T (δ 7.56) and the HC(8) proton of 5′-G (δ 7.94) were also broadened. Upon further addition of **3** (total 10 mM, two equimolar amounts) (Figure 7c), the shift of the CH_3−C(5) protons (3′-T) to 2.15 was completed. The HC(6) (3′-T) and HC(8) (5′-G) also completely shifted to 7.98 and 7.86, respectively. It was thus concluded that the 2:1 $(ZnL')_2$−GpT$^-$ complex **11** was inert and stable at [GpT] = 5 mM and [**3**] = 10 mM at pH 8.[37] A similar downfield shift of the HC(6) (3′-T) was observed in the 2:1 $(ZnL')_2$−T$^-$pT$^-$ complex **8** (see Figure 6c). Therefore, we speculate that the 3′-T ring was orthogonal to an acridine ring. The overall structure of the $(ZnL')_2$−GpT$^-$ complex **11** may be similar to **8**. The formation of the 2:1 complex **11** was further supported by the following FAB mass spectral study.

(37) ZnL′−G complex part in **11** may include the guanine N(1) amide-deprotonated form (see ref 28).

When CpT (5 mM) was mixed with **3** (5 mM), the upfield shifts were seen of CH_3−C(5) and HC(6) of 3′-T from δ 1.89 to 1.60 and from δ 7.70 to 7.27, respectively (Supporting Information). These shift patterns were similar to those for the 1:1 complex of dT and **3**. The doublet HC(6) proton of 5′-C shifted from δ 7.83 to 7.67. The above UV titration and the following FAB mass results confirmed the formation of the 1:1 ZnL′−CpT$^-$ complex **9**, but not a 2:1 $(ZnL')_2$−CpT$^-$ complex.

The mixture of ApT (5 mM) with **3** (5 mM) showed the downfield shift for CH_3−C(5) of 3′-T from δ 1.66 to 1.76 (Supporting Information). The protons HC(8) and HC(2) of 5′-A shifted upfield from δ 8.30 and 8.18 to δ 7.89 and 7.72, respectively. A further addition of **3** (total 10 mM) did not cause any further shift in these signals. It was concluded that only a 1:1 ZnL′−ApT$^-$ complex **10** was formed, which was supported by the UV titration and the following FAB mass results.

The Stoichiometry of 1:1 and/or 2:1 Complexes by FAB-MS (Positive Mode) Measurements. Since all the attempts to isolate the complexes of ZnL′ **3** with dinucleotides failed, the 1:1 and/or 2:1 complex formation was proven by FAB-MS (positive mode) measurements of 1:1 or 2:1 ZnL′/dinucleotide at pH 8 in aqueous solution.

In the 1:1 ZnL′/TpTmixture, we observed major peaks at *m*/*z* 973, 997, and 1402 with each having Zn isotopic peaks, which were ascribed to the complex formations of $[(ZnL')^{2+}-(T^-pT)^{2-}\cdot H^+]^+$ (*m*/*z* 974.31), $[(ZnL')^{2+}-(T^-pT)^{2-}\cdot Na^+]^+$ (*m*/*z* 996.29), and $[((ZnL')_2)^{4+}-(T^-pT^-)^{3-}]^+$ (*m*/*z* 1401.17), respectively. In the 2:1 ZnL′/TpT mixture, we observed a major peak at *m*/*z* 1402 with Zn isotopic peaks, which confirmed the exclusive 2:1 complex formation of $[((ZnL')_2)^{4+}-(T^-pT^-)^{3-}]^+$ (*m*/*z* 1401.17).

In the 1:1 ZnL′/GpT mixture, we observed major peaks at *m*/*z* 998 and 1022 with each having Zn isotopic peaks, which fit to the formation of the 1:1 complex, $[(ZnL')^{2+}-(GpT^-)^{2-}\cdot H^+]^+$ (*m*/*z* 999.32) and $[(ZnL')^{2+}-(GpT^-)^{2-}\cdot Na^+]^+$ (*m*/*z* 1021.30), respectively. In the 2:1 ZnL′/GpT mixture, we observed major peaks at *m*/*z* 998, 1024, and 1428 with each composed of Zn isotopic peaks, which supported the formation of the 1:1 complex $[(ZnL')^{2+}-(GpT^-)^{2-}\cdot H^+]^+$ (*m*/*z* 999.32), $[(ZnL')^{2+}-(GpT^-)^{2-}\cdot Na^+]^+$ (*m*/*z* 1021.30), and the 2:1 complex $[((ZnL')_2)^{4+}-(G^-pT^-)^{3-}]^+$ (*m*/*z* 1426.18), respectively.

In the 1:1 and 2:1 ZnL′/CpT mixtures, we observed major peaks at *m*/*z* 958 and 982 with each Zn isotopic peaks, which

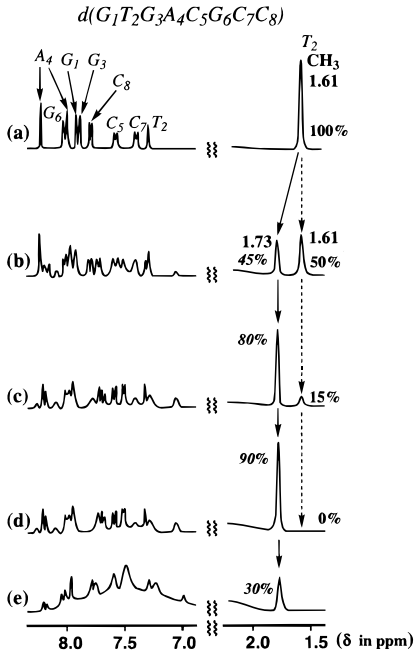

Figure 8. ^{1}H NMR spectra at pD 8.4 and 5 °C in D_2O: (a) 1 mM d(GTGACGCC); (b) 1 mM d(GTGACGCC) + 0.6 mM **3**; (c) 1 mM d(GTGACGCC) + 1 mM **3**; (d) 1 mM d(GTGACGCC) + 1.2 mM **3**; and (e) 1 mM d(GTGACGCC) + 2 mM **3**.

confirmed the formation of 1:1 complex $[(ZnL')^{2+}-(CpT^-)^{2-}\cdot H^+]^+$ (*m*/*z* 959.29) and $[(ZnL')^{2+}-(CpT^-)^{2-}\cdot Na^+]^+$ (*m*/*z* 981.27), respectively. We did not observed any peak for the 2:1 complex.

In the 1:1 and 2:1 ZnL′/ApT mixtures, we observed major peaks at *m*/*z* 982 and 1006 with each Zn isotopic peak, which confirmed the formation of a sole 1:1 complex $[(ZnL')^{2+}-(ApT^-)^{2-}\cdot H^+]^+$ (*m*/*z* 983.32) and $[(ZnL')^{2+}-(ApT^-)^{2-}\cdot Na^+]^+$ (*m*/*z* 1005.30), respectively.

All of these FAB-MS results lent strong support for the conclusions about the ZnL′−dinucleotide complex stoichiometries derived from the potentiometric pH titration, the UV titration, and the NMR studies.

The ^{1}H NMR Spectral Titration of a Single-Stranded Octanucleotide d(GTGACGCC) by ZnL′ (3). Interaction of **3** at various concentrations with a single-stranded octanucleotide d(GTGACGCC) (1 mM) was investigated by the ^{1}H NMR titration at 5 °C in pD 8.4 (Figure 8). When 0.6 mM of **3** was added, 50% intensity of $CH_3-C(5)$ (δ 1.61 ppm) of the original T decreased and a new peak appeared at 1.73 ppm with 45% intensity (see Figure 8b), which was assigned to $CH_3-C(5)$ of **3**-bound T^- (i.e., d(G(ZnL′−T^-)GACGCC)). We have seen the similar downshift of the $CH_3-C(5)$ peak of the **3**-bound T^- in the 2:1 $(ZnL')_2-GpT^-$ complex **11**. When 1.0 mM **3** was added, 80% of the d(GTGACGCC) was bound to **3** at the T base (see Figure 8c). When excess amounts of **3** (1.2 mM) were added, 90% d(G(ZnL′−T^-)GACGCC) was formed, and $CH_3-C(5)$ of the original T completely disappeared (see Figure 8d). When 2 mM of **3** was added, $CH_3-C(5)$ of the **3**-bound T^- decreased to 30% and almost aromatic protons for d(GTGACGCC) broadened, suggesting that the excess **3** randomly interacted with the other bases (e.g., adjacent G's) (see Figure 8e). Finally, when 3.0 mM of **3** was added, the $CH_3-C(5)$ peak of the **3**-bound T^- completely disappeared. It was concluded that at [**3**] < 1.2 mM, ZnL′ preferentially bound to the thymine base in d(GTGACGCC) (1 mM) despite the presence of three guanine bases. The present NMR results with the varying signal intensity of $CH_3-C(5)$ peaks at δ 1.61 and 1.73 (at [**3**] = 0−1 mM) were used to estimate the apparent affinity constant K_{app} (eq 8) for d(G(ZnL′−T^-)GACGCC) complexation. By assuming that the nucleotide was comprised of uncomplexed d(GTGACGCC) and d(G(ZnL′−T^-)GACGCC), the obtained log K_{app} value at pH 8.4 was 4.3 ± 0.2, which agreed fairly well with a corresponding log K_{app} value of 4.9 for $K_{app} = [ZnL'-dT^-]/[\mathbf{3a} + \mathbf{3b}][dT]$.[28]

$$\mathbf{3a} + d(GTGACGCC) \rightleftarrows [d(G(ZnL'-T^-)GACGCC]$$
$$K_{app} = [d(G(ZnL'-T^-)GACGCC)]/[\mathbf{3a} + \mathbf{3b}][d(GTGACGCC)] \quad (8)$$

The ^{1}H NMR Spectral Change in a Double-Stranded Octanucleotide d(CGCTAGCG)$_2$ in the Presence of ZnL′ (3). To see the interaction of **3** with T in a double-stranded d(CGCTAGCG)$_2$, we attempted the similar NMR measurement (at [d(CGCTAGCG)$_2$] = 0.5 and 100 mM $NaNO_3$) at 5 and 25 °C in D_2O at pD 8.4. This double-stranded DNA was often used as a model to study the DNA-interacting drugs.[10,38−42] The ZnL′ **3** (0−3 mM) was gradually added to a solution of 0.5 mM d(CGCTAGCG)$_2$. However, unlike the case of single-stranded d(GTGACGCC), all the proton peaks became broadened too much to be assigned. Note that in all the earlier studies of the DNA-interacting drugs (e.g. distamycin[43−45]), the double-stranded DNA structure became stabilized to give the more sharpened and resolvable NMR spectra upon the complexations,[46−49] whereas in our case, **3** destabilized the double-stranded DNA.

Then, we resorted to measurements of proton exchange rate between solvent H_2O and the imino protons (see Chart 1a) (involved in the hydrogen bonds for the double-strand) of d(CGCTAGCG)$_2$ ([d(CGCTAGCG)$_2$] = 0.5 mM, T_m = 65 °C) in 10 mM HEPES buffer (pH 7.6, D_2O:H_2O = 1:9) with I = 0.10 ($NaNO_3$) at 15 °C. The signal disappearance of the imino protons might measure the degree of interaction of **1** or **3** with octanucleotide duplex, since the interaction would result in rewinding or denaturing of the double helix to accelerate the imino proton exchange rate. The A−T and C−G imino protons in d(CGCTAGCG)$_2$ were assigned according to Hecht's study,[10] where both of the outermost G···C imino protons (2H for (i) and (viii), see Chart 1b) did not show up, due to fast exchange with solvent. The initial integral values of 2H for the A−T ((iv) and (v)) and 4H for C−G ((ii) and (vii); (iii) and (vi)) imino protons decreased and eventually became zero with addition of increasing amounts of **1** (0−5 mM). On the other hand, the Zn^{2+}-free ligand cyclen (1 mM, L·2H$^+$) showed no such effect. A similar effect was observed at lower concentrations with **3**

(38) Manderville, R. A.; Ellena, J. F.; Hecht, S. M. *J. Am. Chem. Soc.* **1994**, *116*, 10851−10852.
(39) Spielmann, H. P.; Wemmer, D. E.; Jacobson, J. P. *Biochemistry* **1995**, *34*, 8542−8553.
(40) Tereshko, V.; Urpí, L.; Malinina, L.; Huynh-Dinh, T.; Subirana, J. A. *Biochemistry* **1996**, *35*, 11589−11595.
(41) Petersen, M.; Jacobsen, J. P. *Bioconj. Chem.* **1998**, *9*, 331−340.
(42) Patel, D. J.; Kozlowski, S. A.; Ikuta, S.; Itakura, K.; Bhatt, R.; Hare, D. R. *Cold Spring Harb. Symp. Quantum Biol.* **1983**, *47*, 197−206.
(43) Klevit, R. E.; Wemmer, D. E.; Reid, B. R. *Biochemistry* **1986**, *25*, 3296−3303.
(44) Pelton, J. G.; Wemmer, D. E. *Biochemistry* **1988**, *27*, 8088−8096.
(45) Pelton, J. G.; Wemmer, D. E. *Proc. Natl. Acad. Sci. U.S.A.* **1989**, *86*, 5723−5727.
(46) Scott, E. V.; Zon, G.; Marzilli, L. G.; Wilson, W. D. *Biochemistry* **1988**, *27*, 7940−7951.
(47) Brown, D. R.; Kurz, M.; Kearns, D. R.; Hsu, V. L. *Biochemistry* **1994**, *33*, 651−664.
(48) Yang, Y.; Huang, L.; Pon, R. T.; Lown, J. W. *Biochem. Biophys. Res. Commun.* **1995**, *212*, 995−1000.
(49) Caceres-Cortes, J.; Sugiyama, H.; Ikudome, K.; Saito, I.; Wang, A. H.-J. *Biochemistry* **1997**, *36*, 9995−10005.

Chart 1

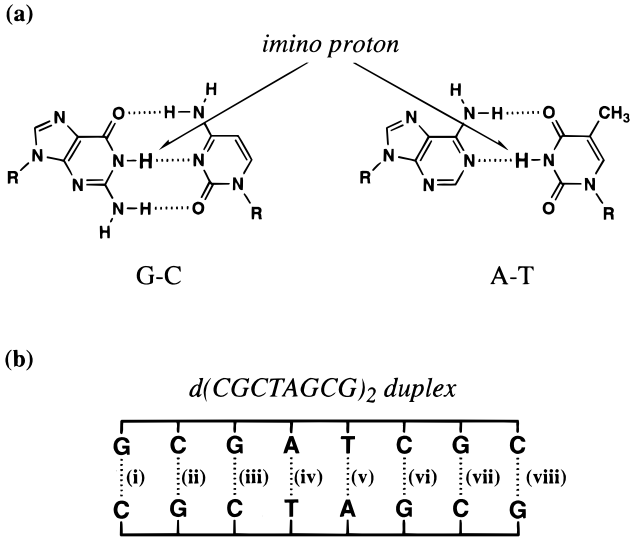

(0−0.5 mM). These observations indicated that the Zn^{2+}−cyclen complexes interacted with DNA, which was facilitated by the pendant acridine group. The effect of the acridine pendant was separately illustrated by the more effective T_m lowering (51 °C → <25 °C with 0.05 mM d(CGCTAGCG)$_2$) by 0.3 mM **3** than 2 mM **1**.[50] Although we saw faster exchange of the imino protons at the A···T sites ((iv) and (v)) and the outer G···C sites ((ii) and (vii)) than the inner G···C sites ((iii) and (vi)), the present NMR data alone unfortunately may not allow us to conclude anything about the preferred binding sites of the Zn^{2+}−cyclen complexes in the double-stranded DNA.

Molecular Modeling of 2:1 (ZnL′)$_2$−T$^-$pT$^-$ Complex 8. To rationalize the cooperative binding of the second ZnL′ **3** to TpT, we attempted to calculate the minimum energy for the 2:1 (ZnL′)$_2$−T$^-$pT$^-$ complex **8** having six conceivable conformations I−VI in aqueous solution (Scheme 6). We have first considered a hypothetical conformation I from the chemical shifts of TpT in the ^{1}H NMR experiment, from which the energy minimization was performed. The computation yielded a converged structure having the most feasible conformation I as depicted in Figure 9. The other hypothetical conformations II−VI were similarly optimized each from the starting structures. However, the conformations IV−VI were immediately transformed to conformation III. Finally, conformation I was found to be the lowest energy structure among all the possible structures for 2:1 (ZnL′)$_2$−T$^-$pT$^-$ complex **8**. The order of stability was conformation I > II > III (i.e., E_{total}(II) − E_{total}(I) = 66.6 kcal mol^{-1} and E_{total}(III) − E_{total}(I) = 116.2 kcal mol^{-1}, see the Experimental Section).

In the most stable conformation I, two pyrimidine rings were completely destacked. The structure of the ZnL′−(5′-T$^-$) part of **8** was similar to the previously elucidated ZnL′-(1-methylthymine$^-$) complex by X-ray crystal analysis.[28] The acridine moiety is face-to-face with the plane of thymine base (5′-T) at an interplane distance of ca. 3.4 Å which is a normal cofacial distance.[28] There was no stacking interaction between the acridine moiety of the second ZnL′ and the thymine base of the (3′-T$^-$) part. However, as we had suspected, there was

(50) The thermal melting curves for the double-stranded d(CGCTAGCG)$_2$ (0.05 mM) in the absence and presence of **1** and **3** were measured by following the UV absorbance change at 260 nm as a function temperature in 10 mM HEPES buffer solution (pH 7.6 and I = 0.10 ($NaNO_3$)). In the absence of Zn^{2+} complexes, the T_m value was 51.0 °C. At [**1**] = 2 mM and [**3**] = 0.3 mM, d(CGCTAGCG)$_2$ denatured at 25 °C.

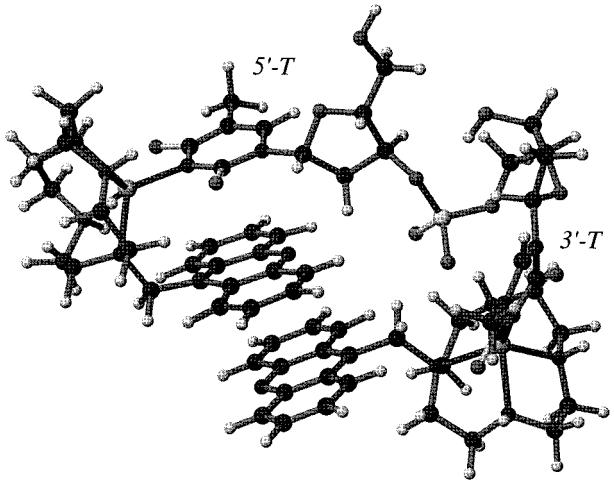

Figure 9. An energy minimized molecular model of the 2:1 (ZnL′)$_2$−T$^-$pT$^-$ complex **8** in aqueous solution.

Scheme 6

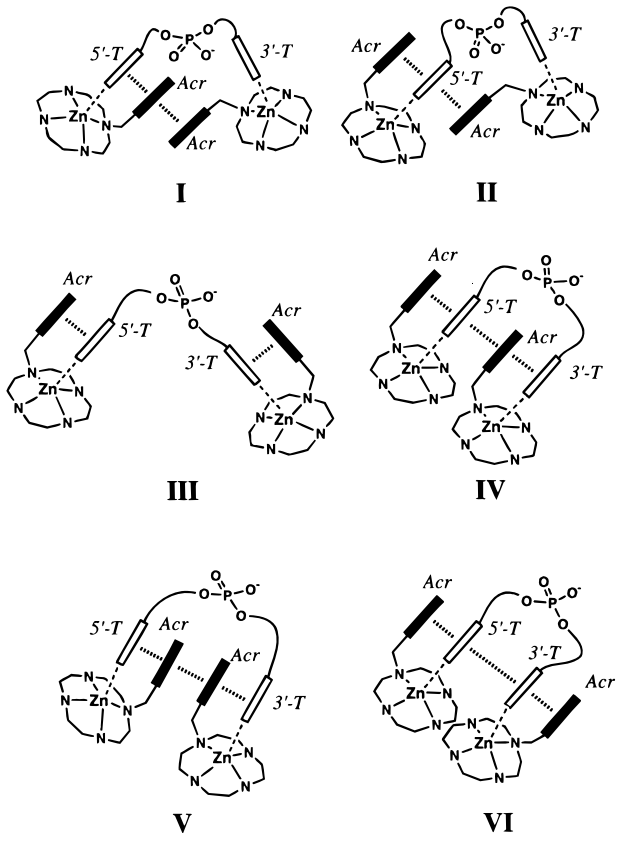

a face-to-face interaction between the two acridine groups (at the interplane distance of ca. 3.6 Å) in the final 2:1 (ZnL′)$_2$−T$^-$pT$^-$ complex **8**. Figure 9 depicts a well-arranged interfacial stacking of the two acridines and the pyrimidine ring of 5′-T. The overlapped position of the pyrimidine ring of 5′-T with the two acridine groups accounted for the aforementioned ^{1}H NMR upfield shifts of the protons on the periphery of the thymine base (5′-T). On the other hand, the perpendicular position of the pyrimidine ring of 3′-T against the two acridine groups accounted for the ^{1}H NMR downfield shifts of the protons on the periphery of the thymine base (3′-T). The intermolecular interactions between the two acridine groups are not strange. For example, in the ZnL′−(1-methylthymine$^-$) complex, an intermolecular stacking was seen, forming a sequence of an intermolecularly stacked pair of thymine (T)

and acridine (Acr) subunits in the order of −T−T−Acr−Acr−.[28] Moreover, in the 2:1 complex of ZnL′ **3** with terephtharate, the intermolecular interactions occurred between the two acridine groups at the closest interplane contact of 3.78 Å.[51]

It is of interest that in structure **8**, the dihedral angle of the two T planes of TpT was about 62°,[52] which was extremely deviated from the two T paralleling planes of TpT in double-stranded DNA. Furthermore, the distance between the two T planes is about 11.2 Å, which is extremely elongated from the usual distance (ca. 3.5 Å) between the two adjacent nucleobases in double-helical DNA. The present result suggests that the cooperative binding of two ZnL′ **3** to two adjacent thymine bases would dramatically distort ordinary single- and double-stranded DNA structure. This fact, along with the much stronger affinity of ZnL′ **3** to TpT than that of ZnL **1**, explains well our previous finding that ZnL′ **3** far more effectively disrupted double-stranded polyA-polyT than ZnL **1**.[29,30] Moreover, the present study will give support to the previous finding that ZnL′ **3** selectively and efficiently bound to T in the AT-rich regions (e.g., TATTTAT in the TATA box) in native DNA to inhibit *micrococcal nuclease* hydrolysis (Scheme 3) or the binding of a transcriptional factor (e.g., the TATA box binding protein).[31,32]

Concluding Remark

The present studies with potentiometric pH titration, UV spectrophotometric titration, and NMR titrations as well as the FAB-MS study have given the first direct evidence for the interaction of Zn^{2+}−cyclen ZnL **1** and Zn^{2+}−acridinylcyclen ZnL′ **3** with the imide-deprotonated thymine T^- in various oligonucleotides. The ZnL′ **3** bound to all the thymines in dinucleotides (TpT, GpT, CpT, and ApT) and single-stranded d(GTGACGCC) with similar 1:1 binding constants (log K_{app}) of ca. 5 at pH 8. ZnL′ **3** bound cooperatively to the two consecutive thymine bases in TpT, with the second ZnL′−T^- interaction being ca. 20 times more favorable than the first ZnL′−T^- interaction. Hence, we saw only the $(ZnL')_2$−T^-pT^- complex **8** and unreacted TpT, rather than the 1:1 ZnL′−T^-pT complex **7** in a 1:1 ZnL′/TpT mixture (>1 mM). The interaction of ZnL′ **3** (1 equiv) was stronger with TpT (0.5 equiv) than with dT (1 equiv). The structure of the $(ZnL')_2$−T^-pT^- complex **8** was proposed on the basis of the NMR study and molecular modeling, as depicted in Figure 9. Excess amounts of ZnL′ **3** bound to G only after most of the T was occupied in GpT and d(GTGACGCC), as shown by the NMR titrations. All the ZnL′−T^- complexes in the dinucleotides and single-stranded DNA were thermodynamically stable and kinetically inert in the NMR time scale at physiological pH. The NMR imino proton exchange measurement showed that the double-stranded $d(CGCTAGCG)_2$ apparently disintegrated upon addition of ZnL **1** and more efficiently by ZnL′ **3**. We are now assured of ZnL′ **3** efficiently binding to the deprotonated thymine (or uracil) base in single- and double-stranded DNA. The present findings on the selective and efficient interaction of the Zn^{2+}−cyclen complexes with nucleobases in DNA at physiological pH will be useful for further development of Zn^{2+}−macrocyclic complexes such as DNA (or RNA) interacting with small molecules for broad applications in nucleic acid biochemistry as well as medicinal chemistry.

Experimental Section

General Information. All reagents and solvents used were of analytical reagent grade (purity >99%) and were used without further purification. All aqueous solutions were prepared with deionized and distilled water. A Good's buffer TAPS (*N*-tris(hydroxymethyl)methyl-3-aminopropanesulfonic acid) and HEPES (2-(4-(2-hydroxyethyl)-1-piperazinyl)ethanesulfonic acid) were commercially available from Dojindo and used without further purification.

Potentiometric pH Titrations. The electrode system (DKK Corporation Multi Channel Ion Meter IOL-40 with a Ross Combination pH Electrode 8102 BN) was calibrated daily as follows: An aqueous solution (50 mL) containing 4.00 mM HCl and 96.0 mM $NaNO_3$ (i.e., $I = 0.10$) was prepared under an argon (>99.999% purity) atmosphere at 25.0 ± 0.1 °C and then the first pH value (pH_1) was read. After 4.00 mL of 0.100 M NaOH was added to acidic solution, the second pH value (pH_2) was read. The theoretical pH values corresponding to pH_1 and pH_2 were calculated: $pH_1' = 2.481$ and $pH_2' = 11.447$, using K_w ($=a_{H^+}{\cdot}a_{OH^-}$) $= 10^{-14.00}$, K'_w ($=[H^+][OH^-]$) $= 10^{-13.79}$, and $f_{H^+} = 0.825$. The corrected pH values ($-\log a_{H^+}$) were obtained using following equations: $a = (pH_2' - pH_1')/(pH_2 - pH_1)$; $b = pH_2' - a \times pH_2$; pH = $a \times$ (pH-meter reading) + b.

The potentiometric pH titrations were carried out with $I = 0.10$ ($NaNO_3$) at 25.0 ± 0.1 °C, where at least two independent titrations were always performed. Deprotonation constants and complexation constants K (defined in the text) were determined by means of the program BEST.[35] The pH σ fit values defined in the program are smaller than 0.02. The obtained constants containing a term of $[H^+]$ were converted to corresponding mixed constants using $[H^+] = a_{H^+}/f_{H^+}$. The species distribution values (%) against pH ($=-\log a_{H^+}$) were obtained using the program SPE.[35]

Solution pH Change Studies. The electrode system was calibrated by the same method for the potentiometric pH titration (see above). Stock solutions of deoxynucleosides (5 mM, 1 mL), oligonucleotides (5 mM, 1 mL), and ZnL′ (50 μM with $I = 0.10$ ($NaNO_3$), including 0.50 mM $ZnSO_4$ to prevent dissociation of ZnL′, 100 mL) were adjusted to pH 7.45 with 0.1 M NaOH solution. A stock solution of deoxynucleoside or oligonucleotide (10 μL) was injected to the ZnL′ solution (2 mL) at 25 °C. The reference experiment was conducted with distilled water (10 μL) in the absence of deoxynucleoside or oligonucleotide, where no pH change was observed. The solution pH values were read every 6 min with continuous stirring under an argon (>99.999% purity) atmosphere. All the experiments were repeated three times and reproducible results were obtained for all.

UV Spectrophotometric Studies. UV spectra were recorded on a Hitachi U-3500 spectrophotometer. The UV absorption (at 362 nm) of **3** (2 mM) with or without dT, TpT, GpT, CpT, or ApT was measured at 25 °C and pH 8.4 (20 mM TAPS buffer, $I = 0.10$ ($NaNO_3$)) with a 1 mm cell ([dT, CpT, ApT, TpT, or GpT] 0, 0.5, 1, 1.5, 2, or 3 mM, respectively).

NMR Experiments. The NMR samples of 5 mM dinucleotides (TpT, GpT, CpT, and ApT) in the presence of **3** were prepared in D_2O at pD 8.4 (99.9 atom % D from Merck), and the pD values in D_2O were corrected for a deuterium isotope effect using pD = [pH-meter reading] + 0.40. A solution of $d(CGCTAGCG)_2$ (1 mM) was prepared in 10 mM HEPES buffer (pH 7.6, D_2O:H_2O = 1:9 with $I = 0.10$ ($NaNO_3$)). A solution of complex **8** was prepared at a concentration of 5 mM TpT and 10 mM **3** in D_2O at pD 8.4.

All ^{1}H NMR (500 MHz) spectra were recorded on a JEOL JNM LA-500 spectrometer with 3-(trimethylsilyl)propionic-*2,2,3,3-d*$_4$ acid sodium salt as an internal reference. For one-dimensional spectra, 32768 points were sampled over a spectral width of 8000 Hz at 25 or 5 °C. COSY spectra (8 ppm sweep width, 1024 points in F2, 512 points in F1, 8 scans per F1 block) were recorded and zero-filled to 2048 × 2048 complex points before Fourier transformation, and the free induction decays were apodized by using a 100%-shifted sine-squared bell in both dimensions. ROESY spectra (8 ppm sweep width, 1024 points in F2, 512 points in F1, 128 scans per F1 block) were recorded with a mixing time of 100 ms and zero-filled in the same way, and FIDs were apodized by using a 30%-shifted sine-squared bell in both.

In the ROESY experiments with 5 mM **8**, the following ROEs were observed: between HC(6) of 5′-T and HC(2′), HC(3′), and HC(5′) (δ 7.13, 2.32 (2.44), 5.01, and 3.80, respectively); between HC(6) of 3′-T and HC(2″), HC(3″), and HC(5″) (δ 8.06, 2.39, 4.75, and 4.30,

(51) Kimura, E.; Ikeda, T.; Shionoya, M.; Shiro, M. *Angew. Chem., Int. Ed. Engl.* **1995**, *34*, 663−664.

(52) Orbell, J. D.; Marzilli, L. G.; Kistenmacher, T. J. *J. Am. Chem. Soc.* **1981**, *103*, 5126−5133.

respectively) at 40 °C. These results suggested that both glycosydic linkages of T^-pT^- in complex **8** were anti form.

FAB-MS Measurements. Fast atom bombardment mass spectra (FAB-MS) were recorded in the positive ion mode with a xenon primary atom beam in conjunction with a glycerol matrix on a JEOL JMS−SX102 mass spectrometer. FAB (positive mode) mass spectroscopy was measured for a 1:1 mixture of **3** (30 mM) with dinucleotides (TpT, GpT, CpT, or ApT, 30 mM) and for a 2:1 mixture of **3** (60 mM) with dinucleotides (30 mM) both in pH 8 aqueous solution.

Molecular Modeling. All calculations were carried out with *InsightII/Discover* version 98.0 software package (MSI, San Diego) on Silicon Graphics workstation O_2. The initial component part of ZnL′ was constructed by use of a crystal structure of the ZnL′ unit of **4**[28] using the *Builder* module. An acridine group in conformations I and II was rotated at ca. 180° around the $N-CH_2Ar$ bond. Both glycosydic linkages for the T^-pT^- unit were constructed for the anti form, based on the ROESY experiments of **8** (see above), and then coordination bonds between zinc(II) ions and imido N^- atoms of T^-pT^- were added. Dihedral constraint of 160−180° for both glycosydic linkages was applied in the following calculations. Nonbonded van der Waals interaction was cut off at 10.0 Å, using a fifth-order polynomial switching function with a spline width of 1.0 Å and a buffer width of 0.5 Å. A dielectric constant of 80 and an effective radius of 1.8 Å for water (solvent) were used. The obtained starting structures were initially subjected to 1000 steps of conjugate gradient minimization followed by the molecular dynamics stage (0.5 fs time step) with the CVFF force field[53] and zinc(II) parameters available in the software package. The molecular dynamics calculation was started at 5 K over 1 ps followed by heating over 6 ps at 800 K. The system was maintained at 800 K over 16 ps, gradually cooled to 300 K over 7 ps, and maintained at 300 K over 30 ps. Coordinate values were stored every 0.5 ps for the last 5 ps and then averaged. The averaged structure was subjected to 100 iterations of steepest descent minimization followed by conjugate gradients minimization to yield the final structure, where the root-mean-square derivative for the system was less than 10^{-4} kcal mol^{-1} $Å^{-1}$. A similar calculation for a ZnL′ complex with the 1-methylthymine anion gave a likely structure which is almost the same as that determined by X-ray crystal analysis.[28]

The energy terms (kcal mol^{-1}) for the final structures are bond (E_{bond}), angle (E_{angle}), torsion (E_{tor}), out-of-plane (E_{op}), van der Waals (E_{vdw}), electrostatic (E_e), and hydrogen bond (E_{hb}): $E_{total} = -217.5$ kcal mol^{-1} for conformation I ($E_{bond} = 12.5$, $E_{angle} = 69.7$, $E_{tor} = 34.7$, $E_{op} = 0.4$, E_{vdw}, $= 34.0$, $E_e = -358.0$, and $E_{hb} = -10.8$); $E_{total} = -150.9$ kcal mol^{-1} for conformation II ($E_{bond} = 32.0$, $E_{angle} = 90.6$, $E_{tor} = 48.4$, $E_{op} = 1.4$, E_{vdw}, $= 17.5$, $E_e = -334.0$, and $E_{hb} = -6.8$); and $E_{total} = -101.3$ kcal mol^{-1} for conformation III ($E_{bond} = 40.6$, $E_{angle} = 97.7$, $E_{tor} = 65.4$, $E_{op} = 0.2$, E_{vdw}, $= 26.0$, $E_e = -328.0$, and $E_{hb} = -3.2$).

Acknowledgment. We are grateful to the Ministry of Education, Science and Culture in Japan for financial support through a Grant-in-Aid for Priority Project “Biometallics” (No. 08249103) for E.K. and a Grant-in-Aid for Scientific Research (No. 1672089 and No. 12023237) for T.K. H.K. thanks to the Japan Society for the Promotion of Science for Graduate Scholarship. Authors are thankful to Dr. Ryoji Kasai of the Department of Medicinal Chemistry, School of Medicine, Hiroshima University, for FAB-MS measurements.

Supporting Information Available: ^1H NMR spectra of 5 mM CpT in the presence and absence of 1 equiv of **3**, 5 mM ApT in the presence and absence of 1 equiv of **3**, and ^1H NMR spectral changes of the hydrogen-bonded imino protons of the $d(CGCTAGCG)_2$ duplex upon addition of various concentrations of **1** and **3** (PDF). This material is available free of charge via the Internet at http://pubs.acs.org.

JA000083J

(53) Dauber-Osguthorpe, P.; Roberts, V. A.; Osguthorpe, D. J.; Wolff, J.; Genest, M. *Proteins: Struct. Funct. Genet.* **1988**, *4*, 31−47.